9.15

STUDY ON URBAN HEAT ISLANDS IN TOKYO METROPOLITAN AREA USING A METEOROLOGICAL MESOSCALE MODEL INCORPORATING AN URBAN CANOPY MODEL

Ryozo Ooka*, Kazuya Harayama**, Shuzo Murakami***, Hiroaki Kondo****

*Institute of Industrial Science, University of Tokyo, Tokyo, Japan

**Yamatake Corporation, Tokyo, Japan

***Faculty of Science and Technology, Keio Gijuku University, Yokohama, Japan

****National Institute of Advanced Industrial Science and Technology, Tsukuba, Japan

1. Introduction

The temperature increase due to urbanization, i.e. urban heat islands, is becoming very serious in Japanese cities. Urban heat island phenomena have been analyzed by many researchers. The three-dimensional meteorological meso-scale model is often used to solve the mechanism of urban heat islands [1,2]. On the meso-scale analysis, which was originally developed in order to predict the climate above the surface boundary layer, a one-dimensional heat balance model is usually used for the ground boundary conditions. In this conventional model, a roughness parameter is employed in order to present the effect of the building complex. As the vertical grid size adjacent to the ground surface must be made several times larger than the roughness length in the conventional model, physical phenomena within the surface layer cannot be estimated. Furthermore, the definition of surface temperature is quite vague in the conventional model because its relationship with ground, roof and wall surface temperatures is unclear. Therefore, it is necessary to include the effect of urban canopy exactly in order to analyze the thermal environment at pedestrian level in an urban area. On the other hand, the one-dimensional urban canopy model is also used commonly to analyze urban thermal environments [3,4]. Although this model can predict thermal the environment at pedestrian level easily, it is not possible to consider the effect of local climate due to the assumption of a horizontally homogeneous flow and temperature field.

In this study, a meteorological meso-scale model based on the Mellor-Yamada model level 2.5 [5] which incorporates the urban canopy model proposed by Kondo et al [3] as the boundary conditions (see Fig.1) is developed to bridge the urban climate and urban thermal environment.

2. Incorporating the Urban Canopy Model into the Meteorological Meso-scale Model

The following five factors due to the building complex are incorporated into the meteorological meso-scale model : (1) wind reduction by the building complex, (2) production of turbulence by the building complex, (3) solar radiation heat transfer inside and outside of the building complex, (4) long wave radiation heat transfer inside and outside of the

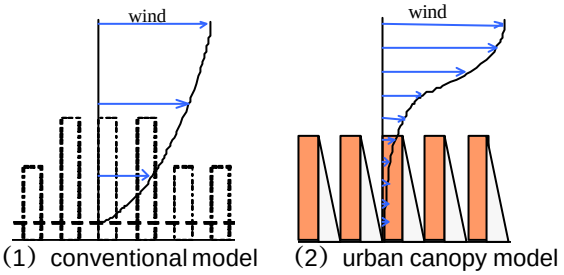

(1) conventional model (2) urban canopy model

Fig. 1 The concept of urban canopy model

* *Corresponding author address*: Ryozo Ooka, IIS, University of Tokyo, 4-6-1 Komaba, Meguro-ku, Tokyo, Japan, e-mail: ooka@iis.u-tokyo.ac.jp

building complex and (5) sensitive and latent heat transfer from the building surface. The four factors due to plant canopy are also incorporated into the meteorological meso-scale model: (1) wind reduction by the plant canopy, (2) production of turbulence by the plant canopy, (3) solar radiation absorption by the plant canopy and (4) transpiration from the plant canopy. These processes are explained as below.

2.1 Modeling the Building Complex.

The effects of the building complex are incorporated into the meteorological meso-scale model as additional terms. In this analysis, a uniform city block, i.e. a series of buildings with the same height (h) , width (b), and interval (w), is assumed within each grid in the meso-scale analysis as shown in Fig. 2. The three-dimensional detailed digital map information system is also utilized to represent the properties of the real building complex, such as the building height, width, and interval. The shapes of the building complex are measured by an airborne laser scanner. Fig. 3 shows the distribution of building height and building width (averaged within a 2km × 2km grid) in Tokyo city area obtained from a Digital Surface Model (DSM) and a Digital Elevation Model (DEM).

2.2 Effect of the Building and Plant Canopy on the Flow Field

The underlined term is added to the following momentum equation for the resistance of the building and plant canopy, referring to the forest canopy model proposed by Yamada [6].

$$\frac{DU}{Dt} = f\left(V - V_g\right) - g\frac{\overline{H} - z^*}{\overline{H}}\left(1 - \frac{\left\langle \Theta_v \right\rangle}{\Theta_v}\right)\frac{\partial z_g}{\partial x} + \frac{\partial}{\partial x}\left(K_{xx}\frac{\partial U}{\partial x}\right) + \frac{\partial}{\partial y}\left(K_{xy}\frac{\partial U}{\partial y}\right) + \frac{\overline{H}}{H - z_g}\frac{\partial}{\partial z^*}\left(-\overline{uw}\right) - \underline{hC_d aU\sqrt{\left(U^2 + V^2 + W^2\right)}} \quad (1)$$

, where h is the ratio of the city block or planting area to the grid area, C_d is the drag coefficient and a is the building or leaf area density. In the building canopy, the building area density a is assumed as $4b/(w+b)^2$.

The underlined terms are added to the following turbulent energy $q^2/2$ and turbulent length scale q^2l equations respectively.

$$\frac{D}{Dt}\left(\frac{q^2}{2}\right) = \frac{\partial}{\partial x}\left[\frac{K_{xx}}{s_q}\frac{\partial}{\partial x}\left(\frac{q^2}{2}\right)\right] + \frac{\partial}{\partial y}\left[\frac{K_{yy}}{s_q}\frac{\partial}{\partial y}\left(\frac{q^2}{2}\right)\right]$$

$$+\left(\frac{\overline{H}}{H - z_g}\right)^2\frac{\partial}{\partial z^*}\left[\left(qlS_q\right)\frac{\partial}{\partial z^*}\left(\frac{q^2}{2}\right)\right] - \frac{\overline{H}}{H - z_g}\left(\overline{uw}\frac{\partial U}{\partial z^*} + \overline{vw}\frac{\partial V}{\partial z^*}\right)$$

$$- b_V g\overline{wq_v} - \frac{q^3}{B_1 l} + \underline{hC_d a\left(U^2 + V^2 + W^2\right)^{\frac{3}{2}}} \quad (2)$$

$$\frac{D\left(q^2 l\right)}{Dt} = \frac{\partial}{\partial x}\left[\frac{K_{xx}}{s_t}\frac{\partial\left(q^2 l\right)}{\partial x}\right] + \frac{\partial}{\partial y}\left[\frac{K_{yy}}{s_t}\frac{\partial\left(q^2 l\right)}{\partial y}\right] + \left(\frac{\overline{H}}{H - z_g}\right)^2\frac{\partial}{\partial z^*}\left[\left(qlS_l\right)\frac{\partial\left(q^2 l\right)}{\partial z^*}\right]$$

$$-lF_1\left[\frac{\overline{H}}{H - z_g}\left(\overline{uw}\frac{\partial U}{\partial z^*} + \overline{vw}\frac{\partial V}{\partial z^*}\right) + b_V g\overline{wq_v}\right] - \frac{q^3}{B_1}\left[1 + F_2\left(\frac{l}{kz}\right)^2\right]$$

$$+ \underline{2hC_d al\left(U^2 + V^2 + W^2\right)^{\frac{3}{2}}} \quad (3)$$

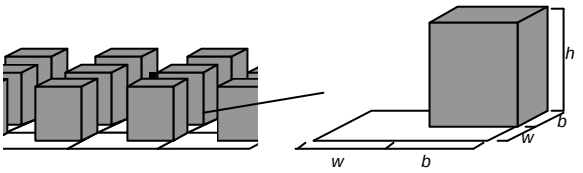

Fig.2 Modeling the Building Complex

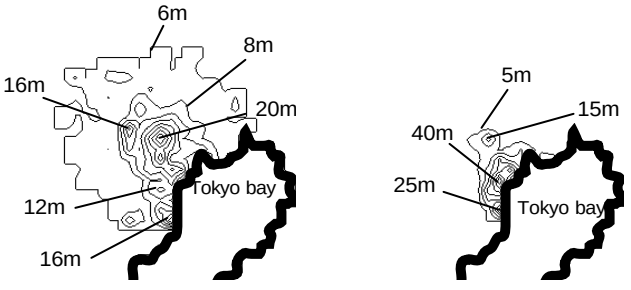

(1) building height (2km grid average)

(2) building width (2km grid average)

Fig.3 Distribution of building height and width in Tokyo

2.3 Effect of the Building and Plant Canopy on the Radiation Field

In order to incorporate the effect of the building canopy on the radiation field, it is necessary to consider complex radiation heat exchange between the ground surface, roof surface, wall surface, and sky. The authors have developed an estimation method based on the Monte Carlo Simulation to analyze the radiant heat transfer in complex urban areas [7]. While this method is expected to give a highly accurate estimation, it is not suitable to be used as a sub-model of the meteorological meso-scale model here, because it increases the computational load. Therefore, an improved and simplified method based on Kondo et al. [3] is adopted in this paper as a relatively simple urban radiation heat transfer model.

2.4 Modeling of the Air-Conditioning Exhaust Heat

In this research, the building energy model shown in Fig.3, are also incorporated into the building canopy model in order to estimate the exhaust heat from air conditioning in the buildings. The building energy model is developed for both commercial and residential buildings. Usually, the air-conditioning heat load is composed of (1) the heat load through the walls, (2) the heat load through the windows, (3) the heat load due to ventilation, and (4) the heat load due to internal heat generation in the building. This air-conditioning heat load is released with the energy consumed by the air-conditioner from air-conditioner's external unit. The ratio of the air-conditioning area to total floor area of a building is assumed to be 0.4 and 0.6 for commercial and residential buildings respectively. The heat load through the walls is obtained by calculating the one-dimensional heat

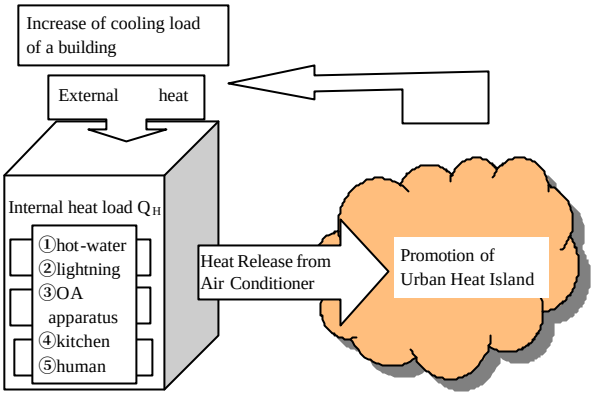

Fig.4 Schematic View of Building Energy Model

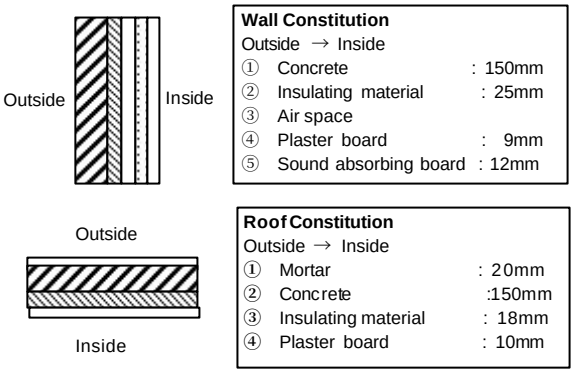

Fig.5 Constitution of Wall and Roof

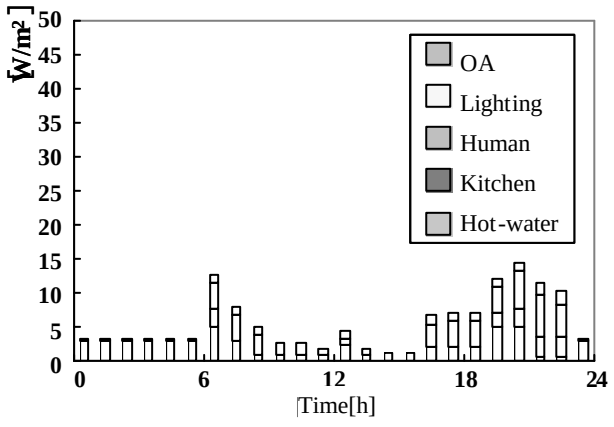

(1) Residential Building

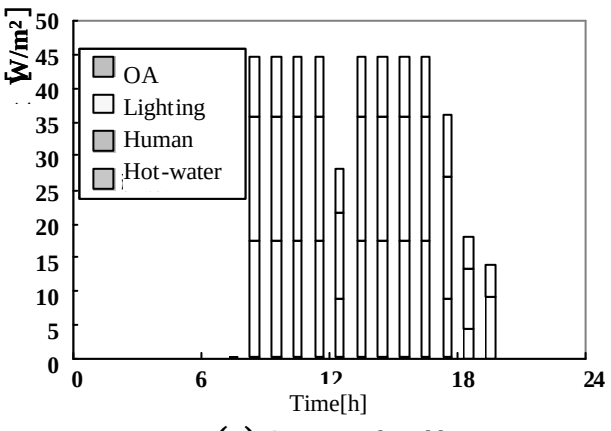

(2) Commercial Building

Fig. 6 Internal Heat Generation per Unit Floor Area [W/m^2]

conduction of the wall. The heat load through the windows is calculated from the transmission of solar radiation through the walls. The ventilation rate is assumed to be 1.1×10^{-3} m^3/m^2s and 3.5×10^{-4} m^3/m^2s for commercial and residential buildings respectively. The heat load due to ventilation is calculated under the condition that the room air temperature and relative humidity are maintained at 26 ℃ and 50% respectively. The internal heat generation per unit floor area in the building is shown in Fig. 6 for commercial and residential buildings.

3. Outline of Analysis

3.1 Analysis Domain

Fig. 5 illustrates the analysis domain which covers 480 km (east-west) × 400 km (south-north) ×9.6 km (vertical direction). The whole analysis domain (grid A) is nested into two sub-domains; grid B and grid C as illustrated in Fig.5. Table 1 also summarized the size and grid discretization of each domain.

3.2 Meteorological Meso-scale Model

The Mellor-Yamada model level 2.5 [5] is employed for meteorological meso-scale analysis in this paper. The urban canopy model described above is incorporated into this analysis.

3.3 Analysis Condition

In this paper, analysis is conducted for the thermal environment on 24th July 1995, which represents a typical summer meteorological situation. The simulations are started from 6:00 a.m. on July 23, and time integration is performed for 42 hours. The initial wind direction and velocity are set southerly 2.0m/s at a height of 9.6km from the ground surface in the whole computational domain. Here, the ground surface is classified into 12 types of land use, and surface parameters, such as albedo, roughness length z_0, heat capacity, and moisture availability b [9][10] are

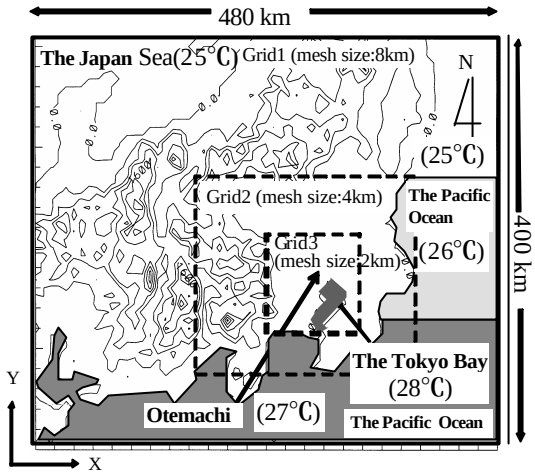

Fig. 7 Analysis Domain

Table 1 Analysis domains and grid arrangements

	Computational Domain (x[km]×y[km]×z[km])	Grid Number	Horizontal Grid Size [km]
Grid1	480×400×9.6	60×50×49	8
Grid2	232×200×9.6	58×50×49	4
Grid3	96×96×9.6	48×48×49	2

Table 2 Surface Parameter

Land Use	Moisture abailavility	Albedo	Roughness length[m]
Rice paddy	0.5	0.20	0.05
Farming	0.3	0.10	0.01
Orchard 1	0.3	0.20	0.05
Orchard 2	0.3	0.20	0.05
Forest	0.3	0.15	0.05
Vacant land	0.3	0.20	0.01
Buildings	0.0	0.10	0.05
Paved Road	0.0	0.10	0.01
Other land	0.0	0.10	0.01
River site	1.0	0.03	0.001
Coast	0.6	0.25	0.005

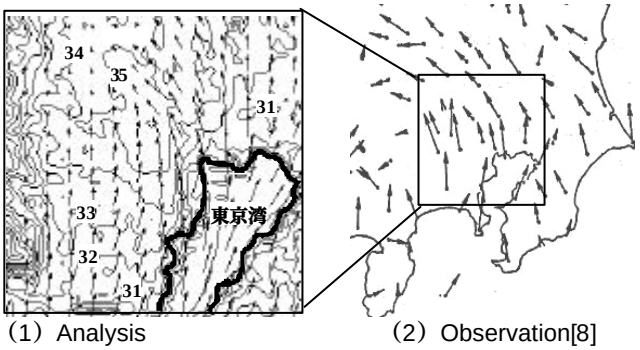

(1) Analysis (2) Observation[8]

Fig. 8 Wind Velocity Vectors (100m height)

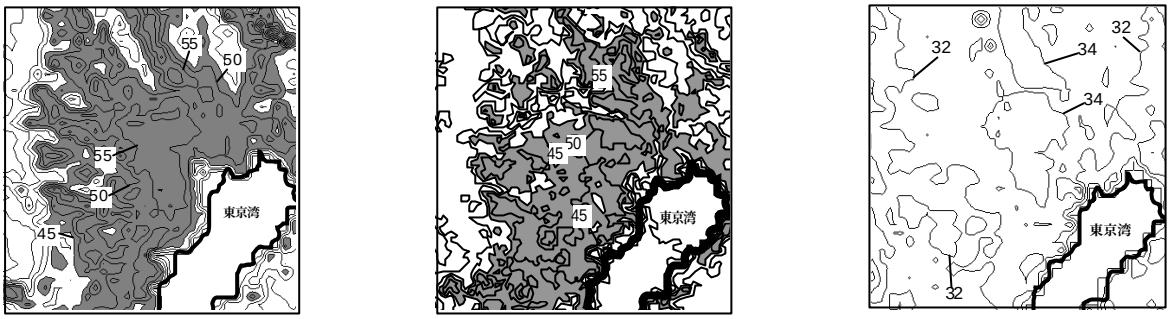

（1）New method (5℃ pitch)　（2）Observation (5℃ pitch)　（3）Conventional method (2℃pitch)

Fig.9　Comparison of surface temperature［℃］(13:00 24th July) (Gray zone shows the areas over 45℃)

set individually following the land use conditions (cf. Table 2).

4. Results and Discussion

Fig.8 shows wind velocity vectors at a height of 100m at 3:00pm. In this simulation, the flow pattern of sea breeze is well reproduced. The correspondence with the measured data is fairly good. Fig.9 shows a comparison of surface temperature between the new method, observation from an artificial satellite and the conventional method employing the one-dimensional heat balance model as the ground boundary conditions. The results of the new method developed here show good agreement with observation compared to those of the conventional method. Fig. 10 shows diurnal variations in the air temperature at a height of 2m in Otemachi in the central part of Tokyo. The analysis results show good agreement with the observation. Fig. 11 shows diurnal variations in the

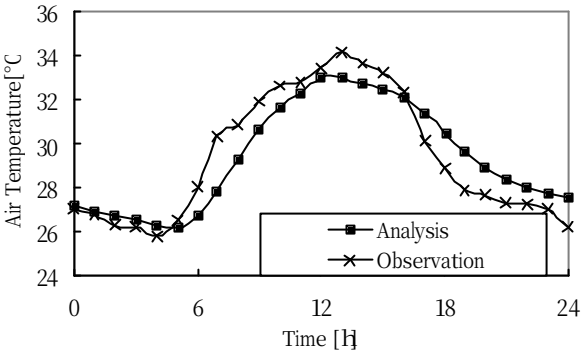

Fig. 10 Diurnal variation of air temperature (2m height, Otemachi)

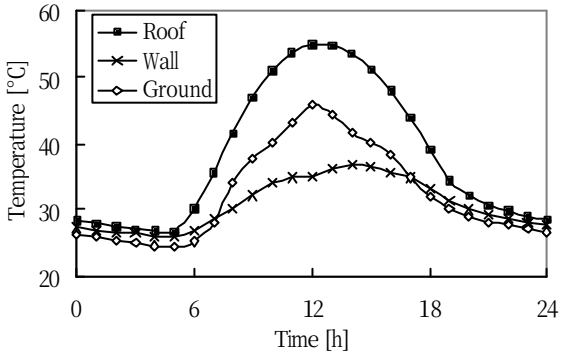

Fig. 11 Diurnal variation of surface temperature (averaged, Otemachi)

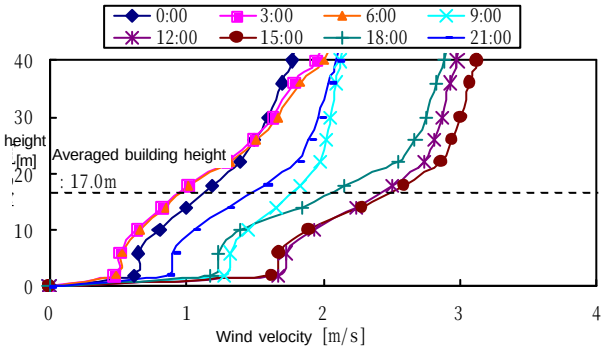

Fig. 12 Vertical Profile of Wind Velocity［m/s］
（24th July, Otemachi）

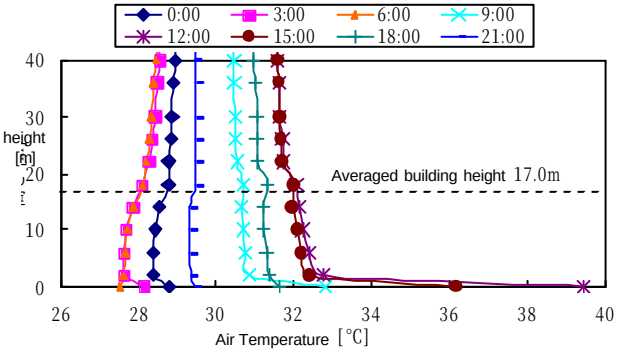

Fig. 13 Vertical Profile of Air Temperature［℃］
（24th July, Otemachi）

surface temperature in Otemachi. Here, the wall surface temperature of a building is the average temperature on all sides of the walls. The roof surface temperature of the building reaches about 55 ℃ around noon. The ground surface temperature is lower than the roof surface temperature, because it is the average of temperature in the sun and in the shade. These surface temperatures can be obtained by introducing the urban canopy model into the meteorological meso-scale analysis. Fig.12 and Fig. 13 show the vertical profiles of the wind velocity and air temperature. The new method developed here can predict physical phenomena inside the urban canopy layer, even in meteorological meso-scale analysis. These results enable us to estimate the thermal environment at pedestrian level. Fig. 14 shows diurnal variation in the heat release air conditioners over the area of 4 km^2 including Otemachi. The method developed in this paper makes it possible to investigate the urban relationship between heat released from air conditioners and urban heat islands.

5. Conclusions

(1) An urban canopy model is incorporated into the meteorological meso-scale analysis method.

(2) Three-dimensional GIS data is used for the Tokyo area in order to identify building complex parameters in the urban canopy model.

(3) The urban canopy model can identify roof, wall and ground surface temperatures in city blocks.

(4) The results of this new method show good agreement with observation.

(5) This new method can estimate the thermal environment at pedestrian level inside the urban canopy layer.

REFERENCES

1. Taha, H., S. Douglas and Jay Haney, Mesoscale meteorological and air quality impacts of increased urban albedo and vegetation, Energy and Building 25, pp.169-177, 1997.

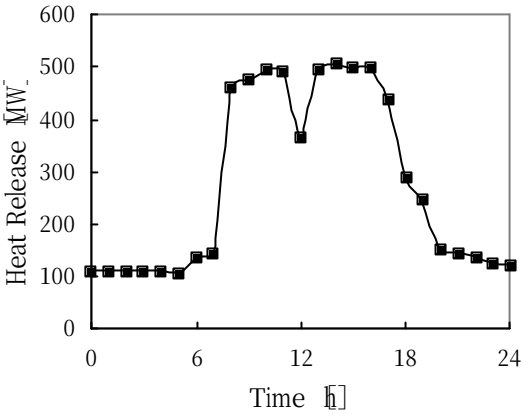

Fig. 14 Diurnal variation of heat release from air conditioner (total in 2km×2km grid, Otemachi)

2. Mochida, A., S. Murakami, T. Ojima, S. Kim, R. Ooka and H. Sugiyama, CFD analysis of mesoscale climate in the greater Tokyo area, Journal of Wind Engineering and Industrial Aerodynamics Vol. 67/68, pp.459-477 , 1997.
3. Kondo, H. and F. Liu, A study on the urban thermal environment obtained through one-dimensional urban canopy model, Journal of Japan Society of Atomospheric Environment, 33 (3), pp.179-192, 1998
4. Ashie, Y., V. T. Ca and T. Asaeda, Building canopy model for the analysis of urban climate, ournal of Wind Engineering and Industrial Aerodynamics Vol. 81, pp.237-248 , 1999.
5. Yamada, T. and S. Bunker, A numerical model study of nocturnal drainage flows with strong wind and temperature gradients, Journal of Applied Meteorology, Vol.28, pp.545-554, 1989.
6. Yamada, T., A numerical model study of turbulent airflow in and above a forest canopy, J of the Meteorological Society of Japan, 439-454, 1982
7. Cheng, H., R. Ooka, K. Harayama, S. Kato and X. Li, Study on outdoor thermal environment of apartment block in Shenzhen, China with coupled simulation of convection, radiation and conduction, Energy and Building, 2004
8. Kuwagata, T. and J. Kondo, Estimation of Aerodynamic Roughness at the regional meteorological stations (AMeDAS) in the Central Part of Japan, TENKI, 37, No.3 55-59, 1990
9. Oue, H., H. Tagashira, K. Otsuki and T. Maruyama, The Characteristics of Heat Balance and Temperature Regime in the Paddy, Potato, Bare Fields and in the Asphalt Area, Trans. JSISRE, 97-104, 1993
10. Fujino, T., C. Shibahara, T. Asaeda, N. Murase, and A. Wake, Characteristics of Heat and Moisture Transport of permeable pavement, Proceeding of Hydrol. Eng., Vol.38, 235-240, 1994